Laser induced single spot oxidation of titanium

Jwad, Tahseen; Deng, Sunan; Butt, Haider; Dimov, Stefan

DOI:
10.1016/j.apsusc.2016.06.136

Document Version
Peer reviewed version

Citation for published version (Harvard):
Jwad, T, Deng, S, Butt, H & Dimov, S 2016, 'Laser induced single spot oxidation of titanium', Applied Surface Science, vol. 387, pp. 617-624. https://doi.org/10.1016/j.apsusc.2016.06.136

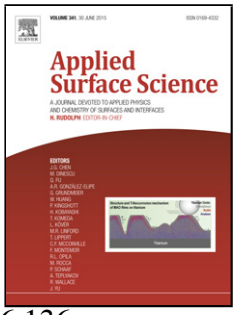

Title: Laser induced single spot oxidation of titanium

Author: Tahseen Jwad Sunan Deng Haider Butt S. Dimov

PII: S0169-4332(16)31365-4
DOI: http://dx.doi.org/doi:10.1016/j.apsusc.2016.06.136
Reference: APSUSC 33506

To appear in: *APSUSC*

Received date: 25-5-2016
Revised date: 21-6-2016
Accepted date: 23-6-2016

Please cite this article as: Tahseen Jwad, Sunan Deng, Haider Butt, S.Dimov, Laser induced single spot oxidation of titanium, Applied Surface Science http://dx.doi.org/10.1016/j.apsusc.2016.06.136

Laser induced single spot oxidation of titanium

Tahseen Jwad[a*], Sunan Deng[a], Haider Butt[a], S. Dimov[a]

[a] *School of Mechanical Engineering, University of Birmingham, Edgbaston, Birmingham B15 2TT, UK*

* *Corresponding author.*
E-mail address: taj355@bham.ac.uk (Tahseen Jwad).

Graphical abstract

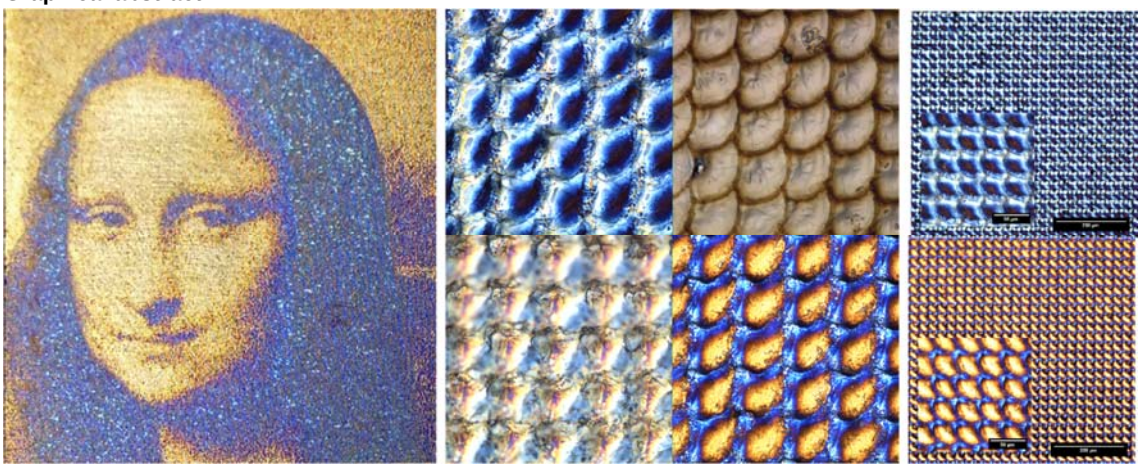

Highlights

- A new high resolution laser induced oxidation (colouring) method is proposed (single spot oxidation).
- The method is applied to control oxide films thicknesses and hence colours on titanium substrates in micro-scale.
- The method enable imprinting high resolution coloured image on Ti substrate
- Optical and morphological periodic surface structures are also produced by an array of oxide spots using the proposed method.
- Colour coding of two colours into one field is presented.

Abstract

Titanium oxides have a wide range of applications in industry, and they can be formed on pure titanium using different methods. Laser-induced oxidation is one of the most reliable methods due to its controllability and selectivity. Colour marking is one of the main applications of the oxidation process. However, the colourizing process based on laser scanning strategies is limited by the relative large processing area in comparison to the beam size. Single spot oxidation of titanium substrates is proposed in this research in order to increase the resolution of the processed area and also to address the requirements of potential new applications. The method is applied to produce oxide films with different thicknesses and hence colours on titanium substrates. High resolution colour image is imprinted on a sheet of pure titanium by converting its pixels' colours into laser parameter settings. Optical and morphological periodic surface structures are also produced by an array of oxide spots and then analysed. Two colours have been coded into one field and the dependencies of the reflected colours on incident and azimuthal angles of the light are discussed. The findings are of interest to a range of application areas, as they can be used to imprint optical devices such as diffusers and Fresnel lenses on metallic surfaces as well as for colour marking.

Keywords: Laser-induced colorizing, titanium oxide, single spot oxidation, color patterning, color coding.

1. Introduction

Titanium (Ti) oxides have received considerable attention by the research community and industry in the last two decades due to its attractive optical and surface properties [1, 2]. In particular, its corrosion resistance, wear resistance, anti-galling properties, biological properties, high strength to weight ratio, good fatigue strength and aesthetic properties (permanent colours) [3], together with Ti mechanical properties [4] are very attractive for a wide range of applications, e.g. photocatalysis, gas sensing, medical implants, optical coatings [5], aerospace and parts identification [3].

Literature review shows that Ti oxide films can be generated by different methods such as heat treatment, immersion in hydrogen peroxide solutions, dipping in rutile and gelatine [6], passivation and anodizing [3]. Although some of these methods are similar and require an immersion of Ti samples into a chemical bath and then to apply DC power, the resulting thickness of the oxide films vary. Another important limitation is that the majority of these treatment methods are nonselective and the resulting oxide thickness is not totally controllable. In addition, high power and wet chemical bath are required, that make them hazardous processes [4].

It is therefore not surprising that oxidation of metals through laser processing is becoming attractive for applications requiring selectivity and high precision [7]. In particular, laser-induced oxidation can offer the following advantages over the other methods:

- Oxidation of pixels/spots with a resolution down to laser wavelength;
- High precision spatial-temporal control;
- Less processing time for relatively small processing areas;
- High repeatability.

Laser-induced colouring of metals can be achieved not only by creating thin films of oxide but also by generating laser-induced periodic surface structures (LIPSS). In particular, different colours were obtained on a range of materials by producing LIPSS employing lasers with pulse durations shorter than the electron-phonon relaxation time (one to tens of picoseconds [8]). LIPSS represents ripples that are usually perpendicular to the laser polarization and diffract light in different colours in the visible range depending on its incident angle. Such periodic surface structures find applications in optical coding [9] and image imprinting [10] and can be generated on a variety of materials such as metals [11-13] and semiconductors [14-16]. In this research only the laser-induced colouring of metals by forming a thin metal oxide layer with nanosecond pulse lasers is studied.

Laser-induced oxidation of different metals has been investigated by many research groups [17] in particular laser-induced colouring of Ti substrates, i.e. the composition and mechanism of laser-induced Ti oxides [5, 18, 19], the structures of Ti oxide films [2, 7], laser-induced colouring versus anodizing [4], and the dependence of colours on laser processing parameters [1, 19-21]. Applications of laser-induced oxidation of metals with its related colouring effects have been considered in jewellery and part identification [22-24]. However, the colourization process reported in the literature was carried out by laser scanning over a relatively large area as compared to the beam spot size. This has limited the applications of the process since the smallest fields of colours that can be produced are in millimetres scale. A comprehensive study of other potential applications has therefore not been carried out, apart from colour marking. The objective of this research is to develop a method to control the size of the oxidation area and its thickness on titanium substrates by laser-induced single spot oxidation and thus to imprint coloured image. By applying this approach the aim is to achieve a pixel resolution down to the beam spot size with high special control in the processed area.

2. Experimental setup

A nanosecond (redENERGY G4 50W) laser from SPI Lasers is used in this research. With wavelength of 1064 nm and a 1 MHz maximum pulse repetition rate, it can be used for laser processing with 25 different pulse durations, from 15 to 220 ns. The beam delivery system used in this experimental study is shown in Figure 1. The 3D scanner (RhoThor RTA) from Newson Engineering can realise scanning speeds of up to 2.5 m/s and the spot size can be controlled down to a few microns in the focal plane with the integrated beam expander and 100 mm telecentric focusing lens. The beam delivery setup is mounted on a mechanical z stage, while the workpiece is horizontally mounted on a high precision stack-up of four mechanical stages (two rotary and two linear Aerotech stages). The beam quality (M^2) is better than 1.3 and the output energy is controlled by an energy attenuator and monitored by an inline power meter. Commercially pure (Grade 1) titanium substrates with a 0.7 mm thickness were used in all the experiments in a temperature-controlled environment. Prior to laser processing, the samples were cleaned ultrasonically for 10 minutes in water and 10 minutes in acetone and dried with hot air. Alicona G5 Infinite Focus (IF) system is used to inspect the morphology of the processed Ti substrates, while the reflectivity measurements along the entire visible spectrum of wavelengths were performed using Ocean Optics USB2000+ Spectrometer with tungsten-filament lighting (CIE illuminant A) and Carl Zeiss Scope A1 optical microscope.

3. Single spot oxidation method

A single spot oxidation method is proposed in this research for a higher resolution than that achievable by applying raster scanning strategies. In addition, by applying this method different topographies can be created on the surface and thus the reflected colours to dependent on the incident and azimuthal angles. Thus, the objective is to achieve a higher resolution down to the beam spot size with high special control in the processed area together with an angular dependence of the colours due diffraction effects.
A single spot of oxide is created on the substrate by a pre-defined number of pulses (a pulse-train processing) that have fluence below the ablation threshold of Titanium. Then, the beam is re-positioned and the next pulse-train is delivered on the substrate and this is repeated until the area that has to be processed is fully covered. In this single spot oxidation method the colour coding is carried out by controlling the number of pulses and fluence, especially the cumulative fluence resulting from each pulse-train.
Initially, arrays of oxide fields were produced on a titanium substrate by applying the proposed single spot oxidation method. Each array included 10 x 10 square fields (2 x 2 mm^2 each) and each square contains (66 by 66) oxidation spots. For producing these arrays, the power is varied from 1% to 100% of the average power (50 W). The distances between any two successive spots in both X and Y directions were fixed at 30 µm while the beam spot size was 80 µm. Thus, the spots overlap. The pulse repetition rate was set to be either 1 MHz or 500 KHz, while the duration time of the pulse-trains was varied from 50 to 214 µs and thus to have trains with different number of pulses, i.e. from approximately 50 to 214 pulses per spot.

A range of colours were generated with the proposed method, i.e. Silver, Golden, Violet, Orange, Blue, and light blue and their variations, that are the same to those reported in the literature which achieved by employing the raster scanning strategy. From the produced initial arrays of oxide fields, 15 fields of colours were selected to produce 6 x 6 mm fields for further analysis. They were selected to cover a wide range of cumulative fluencies and colours but at the same time to minimise the time necessary to carry out the analysis. In particular, Figure 2 depicts these 15 colours, while their laser processing parameters are presented in Table 1. Again, the distances between the spots in both X and Y directions were fixed at 30 µm while the effective spot size is varying from 40 to 80 µm depending on the fluence. The spots' overlaps can be clearly seen in Figure 2.
Figure 3 shows the dependency between the generated colours and cumulative fluence, Cumulative fluence is defined as the average fluence multiplied by the number of pulses and can be calculated as follows [19].

$$F = EN/A = P_{avg}N/AV \quad (1)$$

where: F is cumulative fluence, E - the pulse energy, N - the number of pulses, A - the beam spot area, P_{avg}-the average power, and V-the pulse repetition rate.

Three zones are identified in Figure 3 based on the cumulative fluance levels. In Zone A no colours can be generated because the pulse energy is too low and fluence is below the oxidation threshold (≃ 0.19 J/cm^2) while in Zone C the ablation threshold is exceeded. The oxidation conditions are satisfied in Zone B, especially the cumulative fluence is below ≃ 210 J/cm^2, and thus the colours are changing with the decrease of the cumulative fluence.

4. Results and discussion

In this section the results obtained by applying the single spot oxidation method are presented together with its potential applications.

4.1 Colours parameters

The reflectance spectra of samples 2-15 are shown in Figure 4. They are clustered under three groups based on their cumulative fluence, i.e. 64-93, 98-148, and 180-203 J/cm^2, and their reflectance spectra are shown in Figure 4 (a), (b), and (c), respectively while one reflectance curve from each group is given in Figure 4(d) to compare them.

The Tristimulus values X, Y, and Z, which represent the amounts of the three primary colours, were calculated with Equations 2 to 4 by compensating the values of the colour matching functions ($\bar{x}, \bar{y}, \text{and } \bar{z}$), the illuminate spectral power distribution (S) and the measured reflectance data along the visible wavelength (360-830 nm) based on CIE 1931 [25].Then, the chromaticity coordinates x and y are calculated for each sample and then projected on the CIE1931 two dimensional chromaticity diagram as depicted in Figure 5.

$$X = k \sum_{\lambda} R(\lambda)\, S(\lambda)\, \bar{x}(\lambda)\, \Delta\lambda \quad (2)$$

$$Y = k \sum_{\lambda} R(\lambda)\, S(\lambda)\, \bar{y}(\lambda)\, \Delta\lambda \quad (3)$$

$$Z = k \sum_{\lambda} R(\lambda)\, S(\lambda)\, \bar{z}(\lambda)\, \Delta\lambda \quad (4)$$

$$k = 100 / \sum_{\lambda} S(\lambda)\, \bar{y}(\lambda)\, \Delta\lambda \quad (5)$$

Where:

$R(\lambda)$ Is the reflectance factor,

$S(\lambda)$ - The relative spectral power of a CIE standard illuminant,

$\bar{x}(\lambda)$, $\bar{y}(\lambda)$, and $\bar{z}(\lambda)$ - The colour-matching functions of the CIE standard observers, and

k - The normalising constant

Although CIE1931 and its x-y chromaticity diagram have been used widely in colour industry, their representation in terms of the visual perception is non-uniform. Especially, equal distances in the x-y diagram does not represent an equal magnitude of change in colours [26]. Therefore, the Tristimulus values are converted into L*a*b* and thus to show the colour difference because CIELAB (L*a*b* colour space in CIE 1976) is a uniform colour space and it is recommended when differences in colours have to be represented [27]. The values of L*a*b*, their representations as RGB images, and the photos of all 15 samples are shown in Table 1, where they are ordered by their cumulative fluence.

4.2 **Images imprinting**

A selective oxidation was performed in order to control the oxide thickness of each spot on a Ti substrate. In particular, the single spot oxidation was used to produce pixels of thin oxide films. The films thicknesses and hence the colours are function of beam spot size, burst time, pulse repetition rate and pulse energy. To assess the process capabilities and limitations, an image was imprinted on a titanium substrate. Each pixel of this image was produced with different laser settings, i.e. pulse energy, and thus the oxide thickness was varied. A programme was created in MATLAB to carry out this selective oxidation process. In particular, the programme converts images into executable commands for the laser system. These commands contained the laser parameter settings for each pixel, i.e. power, pulse repetition rate, pulse-train time, and X & Y positions that were set based on the image greyscale map. The pixels were dots with a diameter equal to the beam spot size and thus a high resolution image was imprinted by varying the laser settings. The number of pixels per inch (PPI) can be varied and can go up to 25400/**d**, where **d** is the beam diameter (μm) at the intersection plane with the workpiece. Ultimately, **d** can be reduced down to the laser wavelength with the use of high quality focusing lens that has maximum Numerical Aperture (NA).

To create oxidation patterns on the substrate, two processing strategies were used. The first one was by irradiating the pixels one by one along each row and each column while the second one was a layer-based strategy where the pixels were clustered into one hundred groups (layers) based on their 8-bit representation in the grayscale image. In particular, the 8-bit greyscale image was scaled down from 0-255 to 1-100, where 1 to 100 corresponded to the used average power in percentages, while the pulse repetition rate and train time were kept the same in this experiment at 1 MHz and 0.4 ms, respectively (400 pulses per train). Thus, each layer was produced with different pulse energy and contained all pixels associated with a given group. To imprint an image on a substrate all the layers have to be irradiated one by one.

A 300*300 pixels' image of the Mona Liza was used to carry out imprinting trials figure 6 (f). The image was converted into 300*300 spots and the laser power for each of them was set from 1 to 100% depending on the pixel's 8-bit code. The beam diameter was selected to be 80μm. Thus, the imprinting resolution (pixel density) achieved was 317 PPI while the overall size of the picture was 24 x 24 mm^2. The laser processing time for this image was more than 150 minutes when the first strategy (pixel by pixel processing) was applied. In this case most of the processing time was spent on executing a sequence of 300 x 300 pulse-trains with varying laser processing settings for each pixel. When the layer-based strategy was applied with the same laser settings the processing time was reduced more than seven times, down to less than 20 minutes. However, although the processing time was reduced, the imprinted picture was distorted in some areas. These errors were due to the beam deflectors' dynamics effects when applying the layer-based approach that could be minimised by introducing machine-specific compensations in executing machining vectors [28]. Figure 6 (a-e) shows the image produced with the layer-based strategy on a titanium substrate when the built-in software tool for counteracting the dynamic effects was applied.

This method of imprinting images with permanent colours on Ti substrate can be applied on other types of metals if their oxides have similar properties to Ti oxide such as Niobium, Tantalum, and Chrome, or even on steel. Images in grey scale can be produced by applying this strategy on other types of materials, but then the imprinting mechanism is different. In particular, no oxidation spots are formed but craters are created by applying

pulse energies with fluence higher than the ablation threshold. Craters with different depths can be generated by varying the pulse energy and thus to imprint images with different contrast.

4.3 The angular dependence of the reflected colours

The fields formed by spots of oxides (see Figure 2) reflect different colours when the viewing angle and/or the light incident angle are changed. Inspecting these arrays of single oxidation spots unveiled optical and topographical periodic surface structures because the spots forming them have different profiles/depths, due to the varying oxides' thickness, the beam Gaussian energy distribution and also the spots overlap. All these result in texturing effects on the surface as shown in Figure 2. These periodic surface structures can explain the different colours observed by varying the incident and azimuthal angles. The profile of these structures along a 150 µm line of fields 2 and 14 obtained with Alicona G5 system with 100x objective is given in Figure 7. The periodicity of these structures (peak to peak) is around 32 µm for all inspected samples and this reflects the used constant distance between any two successive spots in applying the proposed single spot oxidation method. At the same time the average amplitude between peaks and valleys is 1.1 to 4.3 µm for these two fields, respectively, that is in line with the different cumulative fluence, 46.96 and 180.1 J/cm^2, used for producing them.

As it was the case with the colours of single spot oxidation arrays, the reflected colours of the imprinted image are dependent on the incident and azimuthal angles, too. In particular, the hair colour of the imprinted image appears blue and black, golden, or light blue depending on the incident and azimuthal angles as shown Figure 6 (a-e). However, the difference here is that the respective area of the imprinted images contains hundreds of spots that were generated using different laser parameter settings and thus resulted in different oxides' topographies and colours. The colours originate from the thin film interference effect produced by the oxide layers while the angular dependence is due to the periodic topographies that results in diffraction effects.

To demonstrate potential applications of this angular dependency, two laser parameters were chosen to process a field of 10*10 mm^2 on a Ti substrate. Single oxidation spots were generated on the substrate by using two different laser parameter settings for the odd and even lines of a field as shown in Figure 8. Note that 20% of the even rows (upper part of the field) have not been processed for the sake of comparison. This phenomena is of interest as it can be used for producing colour coded and colour dependent optical devices on metallic surfaces, such as flat Fresnel lenses, optical diffusers and holograms [29].

5. Conclusions

A method for single spot oxidation is proposed for colourizing/patterning titanium substrates. Different controllable colours were produced on the Ti substrate by generating arrays of single spot oxide films. High resolution images were imprinted to assess the capabilities and also to judge better about potential applications of the proposed method. The fields produced with arrays of single spot oxidations showed an angular dependence of the colours due diffraction effects. This was due to periodic topographies generated with the single spot processing strategy. The findings reported in this paper are of interest to a range of application areas, as they can be used to imprint optical devices such as diffusers and Fresnel lenses on metallic surfaces. Also, images with permanent colours can be imprinted on Ti or other substrates with a resolution up to 25400/**d**.

Acknowledgements

The research reported in this paper was partially funded by the EC FP7 projects: "High throughput integrated technologies for multilateral functional micro components" (HINMICO)' and "Advanced Manufacturing of Multi-Material Multi-Functional Products Towards 2020 and Beyond" (4M2020). The authors would like to thank also the Iraqi Ministry of Higher Education and Scientific Research (MOHESR) for the financial support of Tahseen Jwad's PhD research.

References

[1] L. Skowronski, A.J. Antonczak, M. Trzcinski, L. Lazarek, T. Hiller, A. Bukaluk, A.A. Wronkowska, Optical properties of laser induced oxynitride films on titanium, Appl Surf Sci, 304 (2014) 107-114.
[2] A.J. Antonczak, L. Skowronski, M. Trzcinski, V.V. Kinzhybalo, L.K. Lazarek, K.M. Abramski, Laser-induced oxidation of titanium substrate: Analysis of the physicochemical structure of the surface and sub-surface layers, Appl Surf Sci, 325 (2015) 217-226.
[3] J.C. Puippe, Surface treatments of titanium implants, European Cells and Materials, 5 (2003) 32-33.
[4] A.P. del Pino, J.M. Fernandez-Pradas, P. Serra, J.L. Morenza, Coloring of titanium through laser oxidation: comparative study with anodizing, Surf Coat Tech, 187 (2004) 106-112.
[5] A.P. del Pino, P. Serra, J.L. Morenza, Oxidation of titanium through Nd : YAG laser irradiation, Appl Surf Sci, 197 (2002) 887-890.
[6] R. Rohanizadeh, M. Al-Sadeq, R.Z. LeGeros, Preparation of different forms of titanium oxide on titanium surface: Effects on apatite deposition, J Biomed Mater Res A, 71A (2004) 343-352.
[7] E. Gyorgy, A.P. del Pino, P. Serra, J.L. Morenza, Structure formation on titanium during oxidation induced by cumulative pulsed Nd : YAG laser irradiation, Appl Phys a-Mater, 78 (2004) 765-770.
[8] D. Breitling, A. Ruf, F. Dausinger, Fundamental aspects in machining of metals with short and ultrashort laser pulses, P Soc Photo-Opt Ins, 5339 (2004) 49-63.
[9] J.W. Yao, C.Y. Zhang, H.Y. Liu, Q.F. Dai, L.J. Wu, S. Lan, A.V. Gopal, V.A. Trofimov, T.M. Lysak, Selective appearance of several laser-induced periodic surface structure patterns on a metal surface using structural colors produced by femtosecond laser pulses, Appl Surf Sci, 258 (2012) 7625-7632.
[10] B. Dusser, Z. Sagan, H. Soder, N. Faure, J.P. Colombier, M. Jourlin, E. Audouard, Controlled nanostructrures formation by ultra fast laser pulses for color marking, Opt Express, 18 (2010) 2913-2924.
[11] A.Y. Vorobyev, C.L. Guoa, Colorizing metals with femtosecond laser pulses, Appl Phys Lett, 92 (2008).
[12] P.X. Fan, M.L. Zhong, L. Li, P. Schmitz, C. Lin, J.Y. Long, H.J. Zhang, Angle-independent colorization of copper surfaces by simultaneous generation of picosecond-laser-induced nanostructures and redeposited nanoparticles, J Appl Phys, 115 (2014).
[13] A.R. de la Cruz, R. Lahoz, J. Siegel, G.F. de la Fuente, J. Solis, High speed inscription of uniform, large-area laser-induced periodic surface structures in Cr films using a high repetition rate fs laser, Opt Lett, 39 (2014) 2491-2494.
[14] C.Y. Zhang, J.W. Yao, H.Y. Liu, Q.F. Dai, L.J. Wu, S. Lan, V.A. Trofimov, T.M. Lysak, Colorizing silicon surface with regular nanohole arrays induced by femtosecond laser pulses, Opt Lett, 37 (2012) 1106-1108.
[15] A.A. Ionin, S.I. Kudryashov, S.V. Makarov, L.V. Seleznev, D.V. Sinitsyn, E.V. Golosov, O.A. Golosova, Y.R. Kolobov, A.E. Ligachev, Femtosecond laser color marking of metal and semiconductor surfaces, Appl Phys a-Mater, 107 (2012) 301-305.
[16] H.D. Yang, X.H. Li, G.Q. Li, C. Wen, R. Qiu, W.H. Huang, J.B. Wang, Formation of colorized silicon by femtosecond laser pulses in different background gases, Appl Phys a-Mater, 104 (2011) 749-753.
[17] L. Nanai, R. Vajtai, T.F. George, Laser-induced oxidation of metals: State of the art, Thin Solid Films, 298 (1997) 160-164.
[18] A.P. del Pino, P. Serra, J.L. Morenza, Coloring of titanium by pulsed laser processing in air, Thin Solid Films, 415 (2002) 201-205.

[19] D.P. Adams, R.D. Murphy, D.J. Saiz, D.A. Hirschfeld, M.A. Rodriguez, P.G. Kotula, B.H. Jared, Nanosecond pulsed laser irradiation of titanium: Oxide growth and effects on underlying metal, Surf Coat Tech, 248 (2014) 38-45.
[20] V. Veiko, G. Odintsova, E. Ageev, Y. Karlagina, A. Loginov, A. Skuratova, E. Gorbunova, Controlled oxide films formation by nanosecond laser pulses for color marking, Opt Express, 22 (2014) 24342-24347.
[21] A.J. Antonczak, B. Stepak, P.E. Koziol, K.M. Abramski, The influence of process parameters on the laser-induced coloring of titanium, Appl Phys a-Mater, 115 (2014) 1003-1013.
[22] R. Rusconi, J. Gold, Color marking-High-contrast and decorative effects can be achieved in color on plastics and metals using ND: YAG or Nd: YVO4 lasers, Industrial Laser Solutions-for Manufacturing, 20 (2005) 16-19.
[23] Z. Hongyu, Laser-induced colours on metal surfaces, in, SIMTech Technical Report PT/01/005/AM, 2001.
[24] S. O'Hana, A.J. Pinkerton, K. Shoba, A.W. Gale, L. Li, Laser surface colouring of titanium for contemporary jewellery, Surf Eng, 24 (2008) 147-153.
[25] C. CIE, Commission Internationale de l'Eclairage Proceedings, 1931, in, Cambridge University Press Cambridge, 1932.
[26] S. Westland, C. Ripamonti, Computational colour science using MATLAB, J. Wiley, Hoboken, NJ, 2004.
[27] ISO/CIE, 2011. ISO 11664-4:2011(E)/CIE S 014-4/E:2007 Joint ISO/CIE Standard: Colorimetry — Part 4: CIE 1976 L*a*b* Colour Space. .
[28] P. Penchev, S. Dimov, D. Bhaduri, S.L. Soo, B. Crickboom, Generic software tool for counteracting the dynamics effects of optical beam delivery systems, Proceedings of the Institution of Mechanical Engineers, Part B: Journal of Engineering Manufacture, (2015) 0954405414565379.
[29] H. Butt, Y. Montelongo, T. Butler, R. Rajesekharan, Q. Dai, S.G. Shiva-Reddy, T.D. Wilkinson, G.A. Amaratunga, Carbon nanotube based high resolution holograms, Advanced materials, 24 (2012) OP331-336.

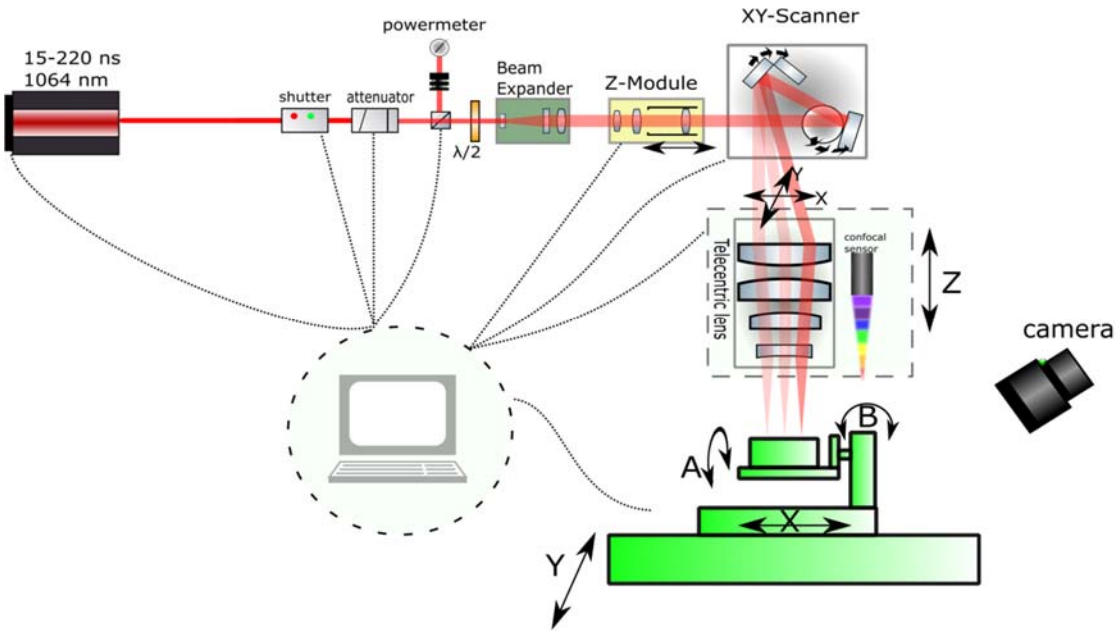

Fig.1. Laser platform setup

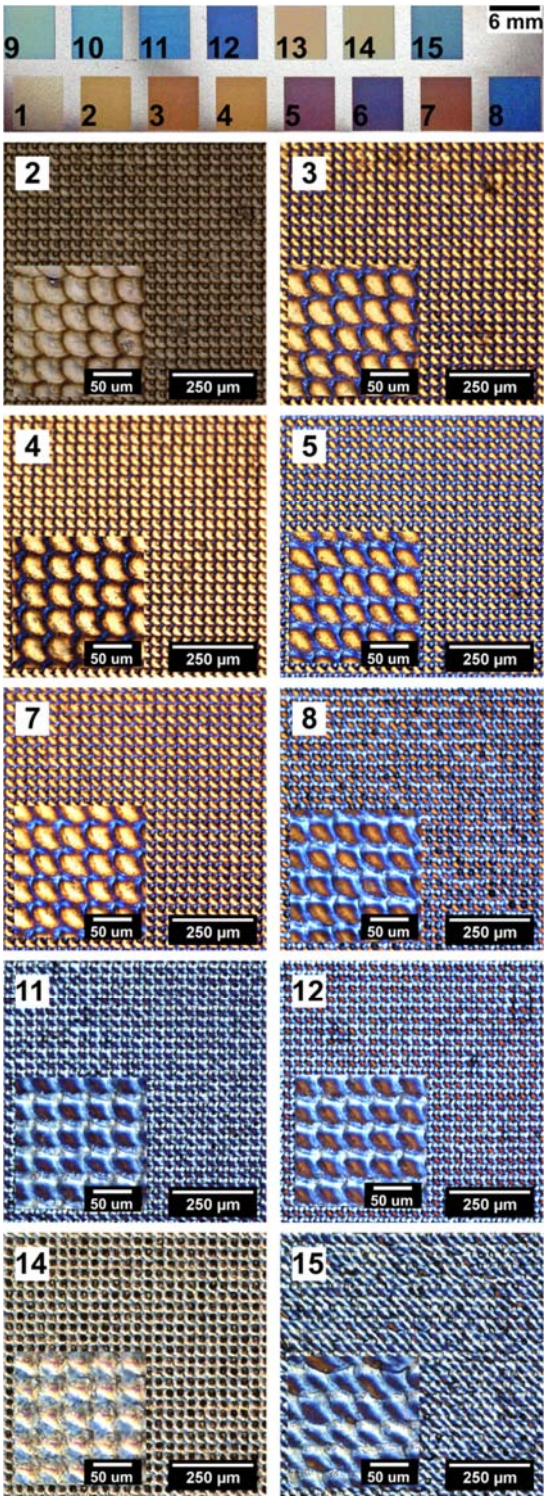

Fig.2. Selected colours generated by single spot oxidation

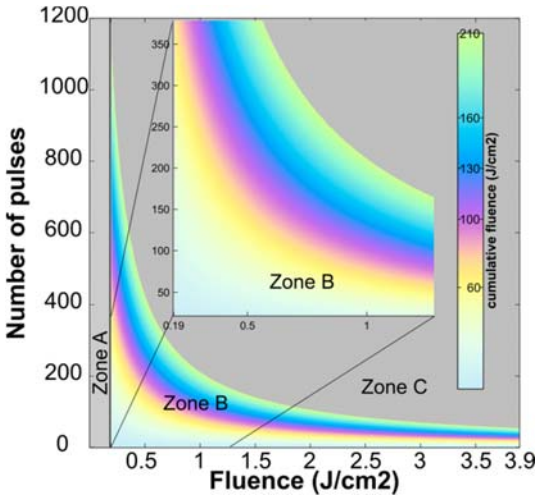

Fig.3. the dependency of the generated colours on the cumulative fluence

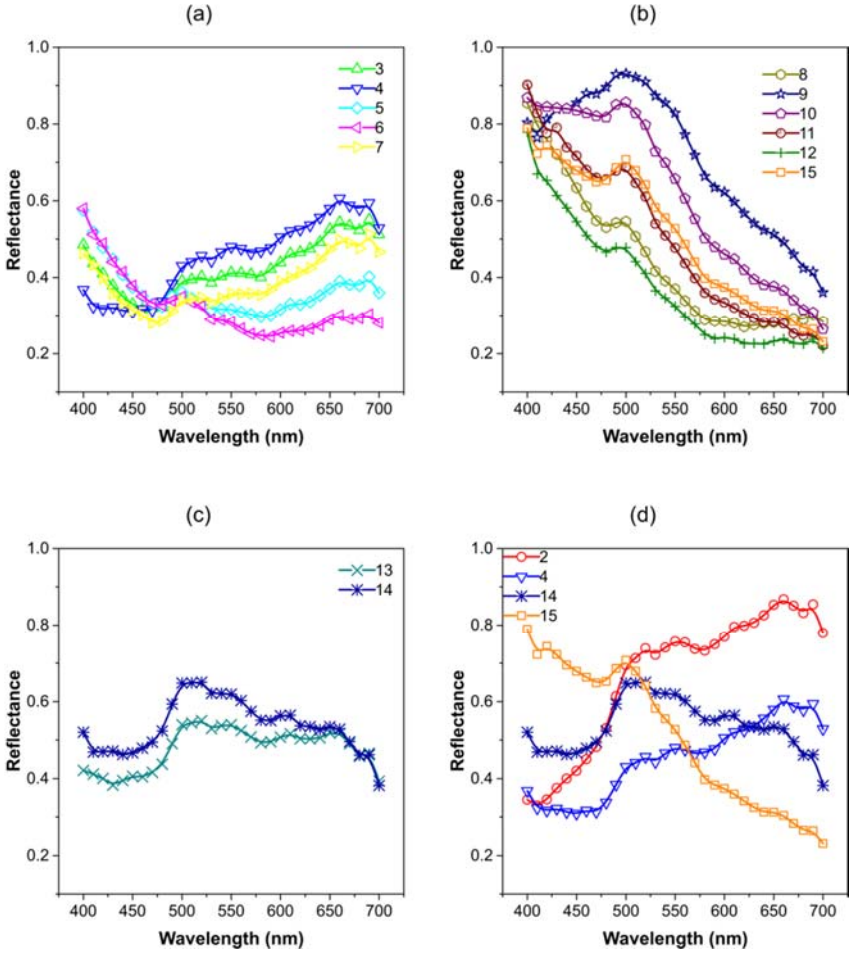

Fig.4. Reflectance spectra of sample 2-15. For samples processed with cumulative fluence 64-93 (a), 98-148 (b) and 180-203 (c) j/cm^2, while (d) combines the reflectance results obtained with the three fluence ranges..

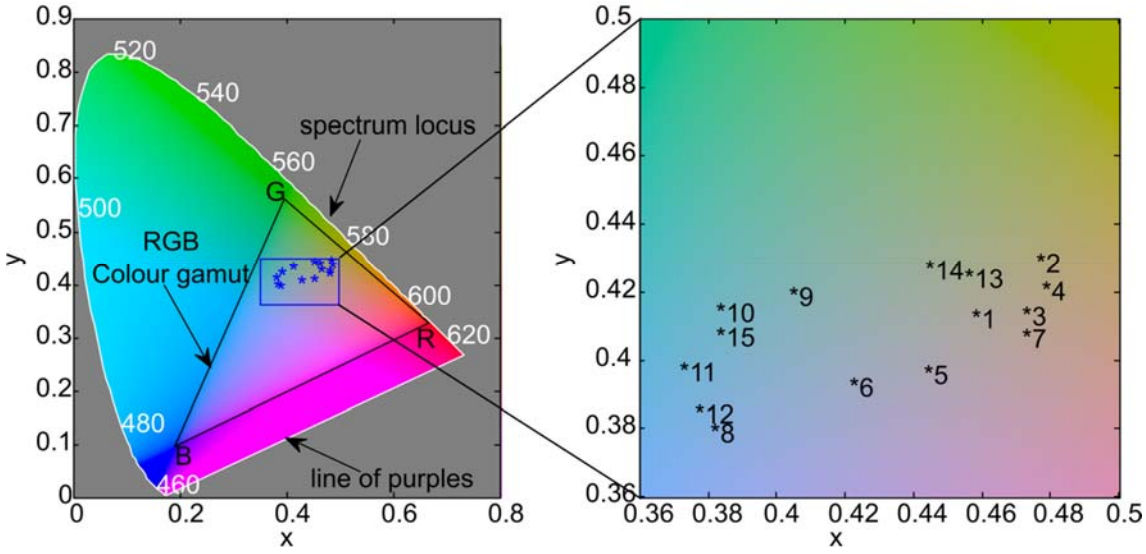

Fig. 5. The chromaticity of 15 samples projected over the CIE 1931 x-y colour space with CIE Illuminant A at Y-tristimulus value of 39 that is the average of Y for the 15 samples).

Note: Y is equal 100 for perfect white surface.

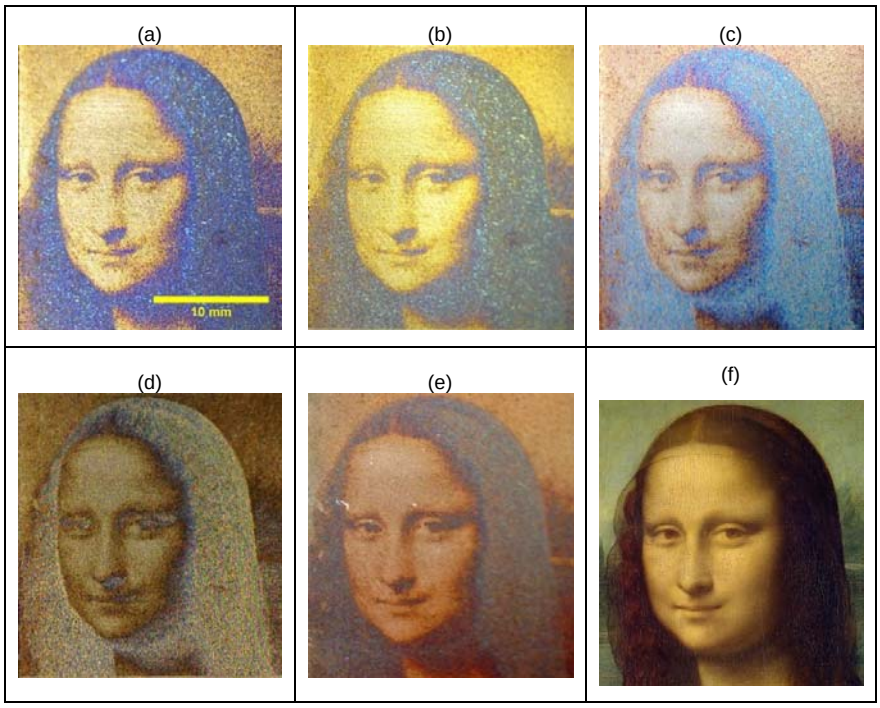

Fig.6. Imprinted image shown in different incident and azimuthal angles. (a) Both normal, (b) different incident, (c –e) different azimuthal angles, while (f) is the original image.

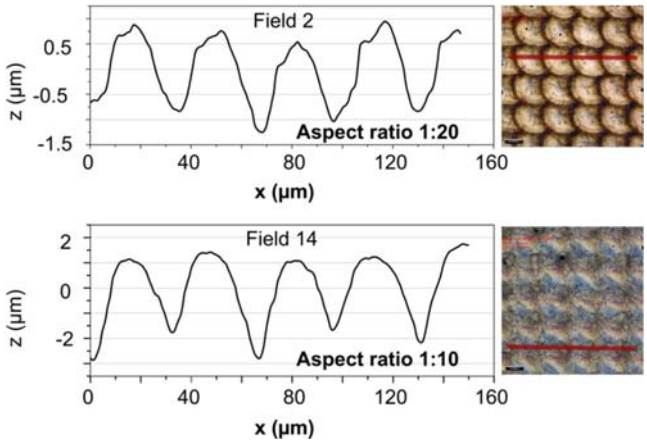

Fig.7. The profiles of the periodic structures for Fields 2 and 14 in Figure 2, respectively

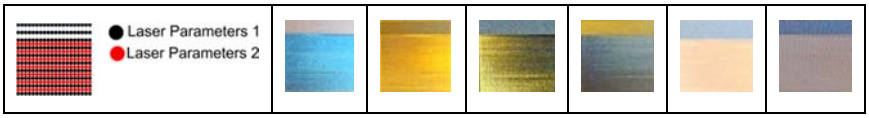

Fig.8. One field coded with two colours using two different laser parameter settings, captured with different incident and azimuthal angles

Table 1 Laser processing parameters, the L*a*b* values, RBG images, and pictures of 15 colours produced by single spot oxidation (sorted by their cumulative fluence)

sample	1	2	4	7	3	5	6	8	12	11	10	15	9	14	13
RGB image															
photo															
L*	97.49	94.27	91.17	87.61	89.77	79.15	73.02	68.92	67.77	73.19	84.32	80.07	90.2	95.43	97.37
a*	1.916	2.166	5.697	8.699	7.199	2.932	-2.43	-11.3	-13.34	-19.48	-22.21	-20.5	-19.08	-8.199	-4.121
b*	6.567	26.77	21.15	9.128	12	-8.210	-16.34	-30.5	-30.28	-28.28	-22.86	-22.7	-11.85	8.849	12.08
PRR (MHz)	1	1	0.5	1	0.5	0.5	0.5	1	1	1	1	0.5	1	1	1
N	50	50	50	75	50	50	50	100	150	150	150	75	150	214	214
BT(μs)	50	50	100	75	100	100	100	100	150	150	150	150	150	214	214
F (J/cm2)	32.13	46.96	64.26	70.44	74.15	84.04	93.93	98.87	103.8	118.6	133.4	140.8	148.3	180.1	203.4

Note: L*a*b* is CIELAB colour space; PRR - pulse repetition rate; N - number of pulses, BT - burst time, F - cumulative fluence